Research Square

Preprints are preliminary reports that have not undergone peer review. They should not be considered conclusive, used to inform clinical practice, or referenced by the media as validated information.

The Memory Effect on Fractional Calculus: An Application in the Spread of Covid-19

Laécio Carvalho de Barros (laeciocb@ime.unicamp.br)
Universidade Estadual de Campinas - Unicamp

Michele Martins Lopes
Universidade Estadual de Campinas - Unicamp

Francielle Santo Pedro Simões
Universidade Federal de São Paulo - UNIFESP

Estevão Esmi
Universidade Estadual de Campinas - Unicamp

José Paulo Carvalho dos Santos
Universidade Federal de Alfenas - Unifal

Daniel Eduardo Sánchez
Universidad Austral de Chile

Research Article

Keywords: Fractional calculus, Hysteresis, Mathematical expectation, SIR model, Covid-19

Posted Date: July 14th, 2020

DOI: https://doi.org/10.21203/rs.3.rs-41084/v1

License: This work is licensed under a Creative Commons Attribution 4.0 International License.
Read Full License

Version of Record: A version of this preprint was published at Computational and Applied Mathematics on March 4th, 2021. See the published version at https://doi.org/10.1007/s40314-021-01456-z.

Noname manuscript No.
(will be inserted by the editor)

The Memory Effect on Fractional Calculus:

An Application in the Spread of Covid-19

Laécio Carvalho de Barros · Michele Martins Lopes · Francielle Santo Pedro · Estevão Esmi · José Paulo Carvalho dos Santos · Daniel Eduardo Sánchez

Received: date / Accepted: date

Abstract Fractional calculus has been widely used in mathematical modeling of evolutionary systems with memory effect on dynamics. The main interest of this work is, through a statistical approach, to attest how the hysteresis phenomenon, which describes the memory effect present in biological systems, can be treated by fractional calculus, and to analyze the contribution of the historical values of a function in the evaluation of fractional operators according their order. In order to illustrate the efficiency of this non-integer order calculus, we consider the SIR (Susceptible-Infected-Recovered) compartmental model which is widely used in epidemiology. We employ SIR models to model the dynamics, with and without memory, of the spread of Covid-19 in some countries.

This work is partially supported by CNPq under grant no. 306546/2017-5 and CAPES.

Laécio Carvalho de Barros
Department of Applied Mathematics, University of Campinas, Campinas, SP, Brazil
E-mail: laeciocb@ime.unicamp.br

Michele Martins Lopes
Department of Applied Mathematics, University of Campinas, Campinas, SP, Brazil
E-mail: mi_martins22@hotmail.com

Francielle Santo Pedro Simões
Multidisciplinary Department, Federal University of São Paulo, Osasco, SP, Brazil
E-mail: fsimoes@unifesp.br

Estevão Esmi
Department of Applied Mathematics, University of Campinas, Campinas, SP, Brazil
E-mail: eelaureano@ime.unicamp.br

José Paulo Carvalho dos Santos
Department of Mathematics, Federal University of Alfenas, Alfenas, MG, Brazil
E-mail: zepaulo@unifal-mg.edu.br

Daniel Eduardo Sánchez
Center of Basic Science Teaching for Engineering, Univ. Austral of Chile, Valdivia, Chile
E-mail: danielsanch@gmail.com

Keywords Fractional calculus · Hysteresis · Mathematical expectation · SIR model · Covid-19

1 Introduction

The fractional calculus was originated in 1695 as a generalization of the integer order calculus. This happened through a question asked by L'Hospital to Leibniz about the meaning of $\frac{d^n}{dx^n}$, being $n = \frac{1}{2}$. In this way, it is possible to define integrals and derivatives with arbitrary orders. Since its inception, many contributions have been made by several researchers, including famous names such as Euler, Lagrange, Laplace, Fourier, Abel and Liouville [1,15].

This calculus is one of the most effective current mathematical tools used to model real-world problems. Several definitions have been proposed for fractional integrals, for example, the fractional integrals of Liouville, Weyl, and Riemann-Liouville. The fractional derivative also has several definitions such as those derived from Riemann-Liouville, Caputo, Liouville, Weyl, Riesz, Grünwald-Letnikov, Marchaud and Hifler [1,12]. In contrast to the Caputo's fractional derivative, most fractional derivative definitions do not satisfy the property that the derivative of a constant is null. This suggests a preference for the Caputo derivative in many situations. Other definitions that are also commonly used today are of Riemann-Liouville and Grünwald-Letnikov, the latter one is more suitable for numerical applications [1,11].

The theory of fractional calculus can be used, among several possibilities, to deal with the memory effect in mathematical modeling. Memory in mathematical modeling makes important what happened in the past to explain the present [1,11]. In [13], a system of fractional differential equations is used to study the effect of memory on epidemic evolution. In [10], the hysteresis effect is used to model biological phenomena that activate defense mechanisms of certain living beings. For example, in a situation of spreading of an infectious disease for human beings, depending on type of disease, previous experiences can reveal that social distance or additional hygiene habits are defensive behaviors to prevent its propagation. The vaccine can also have a long-term memory effect, when it has a lasting effect, causing the body to defend itself through immune memory.

To illustrate the potential of fractional differential equations in epidemiological processes with memory, we investigate the evolution of Covid-19 in a population. Since the spread of COVID-19 occurs through contact between infected individuals and susceptible individuals, with part of the population already recovered, we employ the famous epidemiological SIR (Susceptible-Infected-Recovered) model, which is compartmental model proposed by Kermack and McKrendick in 1927 and is mathematically described by a system of first order differential equations [4]. However, due to the fact that this disease is little known and underreported, parameters such as speed of propagation and recovery and contact rates are difficult to estimate. Consequently, its modeling using classical differential equations can be inappropriate to represent

the dynamics of the populations involved. This is still another justification for adopting fractional equations, since it is possible to adjust the order of the differential equation to the real data of the spread of the disease.

The work is organized as follows. In Section 2, we present some definitions necessary for the mathematical development of the work. Section 3 shows two reasons for the use of fractional calculus, namely, the Tautochrone problem and the memory effect. In Section 4, we present the main results of the work, where we verify objectively the memory effect via statistical tools and analyze the contribution of historical values to the fractional operators. Finally, Section 5 presents the fractional epidemiological SIR model to describe the evolution of Covid-19 in several countries. The numerial experiments reveal how the fractional calculus contributes in the description and modelling of real phenomena. We only seek to compare models with and without memory, with no intention of making predictions about the disease.

2 Preliminary

In this section, we recall some of the main results of the fractional calculus needed in this work.

Definition 1 [8] The improper integral

$$\Gamma(p) = \int_0^\infty e^{-x} x^{p-1} dx, \tag{1}$$

is called the gamma function and it is defined for $Re(p) > 0$, where it is convergent.

Proposition 1 *[8]* The gamma function has the following properties.

a) $\Gamma(p+1) = p\Gamma(p)$;
b) $\Gamma(1) = 1!$;
c) $\Gamma(n+1) = n!$, for $n \in \mathbb{N}$.

Definition 2 (Fractional Integral of Riemann-Liouville [16]) Let $\alpha \in \mathbb{R}^+, b > 0$ and $f \in L^p([0,b] : \mathbb{R}^m)$, with $1 \leq p \leq \infty$. The fractional integral of Riemann-Liouville, for $t \in [0,b]$, of order α, is given by

$$J_t^\alpha f(t) = \frac{1}{\Gamma(\alpha)} \int_0^t (t-s)^{\alpha-1} f(s) ds. \tag{2}$$

When $\alpha \in \mathbb{N}$, we have $\Gamma(\alpha) = \alpha!$. In this case, Equation (2) becomes the Cauchy formula for iterated integrals, which is the motivation for this definition. Furthermore, for $\alpha > 0$ the integral exists for almost every t in $[0,b]$.

We denote by $AC^n[0,b]$ the set of functions in which the order derivative $n-1$ is absolutely continuous in $[0,b]$ [2].

Definition 3 (Fractional Derivative of Riemann-Liouville [16]) Let $\alpha \in \mathbb{R}^+, b > 0$, $f \in AC^n[0,b]$ and $n = \lfloor \alpha \rfloor$. The fractional derivative of Riemann-Liouville of order α is given by

$$D_t^\alpha f(t) = D_t^n J_t^{n-\alpha} f(t) = \frac{d^n}{dt^n}\left(\frac{1}{\Gamma(n-\alpha)}\int_0^t (t-s)^{n-\alpha-1} f(s)ds\right). \quad (3)$$

Definition 4 (Fractional Derivative of Caputo [8,16]) Let $\alpha \in \mathbb{R}^+, b > 0$ and $f \in AC^n[0,b]$. For $t \in [0,b]$, the fractional derivative of Caputo of order α is given by

$$cD_t^\alpha f(t) = D_t^\alpha (f(t) - f(0)). \quad (4)$$

For $\alpha \in (0,1)$, one can show that

$$cD_t^\alpha f(t) = J_t^{1-\alpha} f'(t). \quad (5)$$

Definition 5 (Beta function [8]) The beta function is defined by the integral

$$B(p,q) = \int_0^1 x^{p-1}(1-x)^{q-1}dx, \text{ where } p,q > 0. \quad (6)$$

Proposition 2 *[8]* The gamma and beta functions are related as follows:

$$B(p,q) = \frac{\Gamma(p)\Gamma(q)}{\Gamma(p+q)}. \quad (7)$$

Next, we present some important statistics concepts for the development of the work.

Definition 6 (Beta Distribution [9]) A random variable X follows the beta distribution if its probability density function is given by:

$$f_X(x) = f_X(x;p,q) = \frac{1}{B(p,q)} x^{p-1}(1-x)^{q-1} I_{(0,1)}(x), \quad (8)$$

where $p,q > 0$ and $I_{(0,1)}$ the indicator function of interval $(0,1)$.

Remark 1 When $p = q = 1$ the beta distribution becomes the uniform distribution over the range $(0,1)$.

The expectation or expected value represents the mean of random variable X. Below, we present the definition of this concept for continuous random variable.

Definition 7 [9] Let X be a continuous random variable with the probability density function $f_X(\cdot)$. The expectation or expected value of X is given by

$$E[X] = \int_{-\infty}^{\infty} x f_X(x)dx. \quad (9)$$

Proposition 3 *[9] Let $g : \mathbb{R} \to \mathbb{R}$ and X be a continuous random variable with the probability density function $f_X(\cdot)$. The expectation or expected value of $g(X)$ is given by*

$$E[g(X)] = \int_{-\infty}^{\infty} g(x) f_X(x)dx. \quad (10)$$

3 Motivations for Using Fractional Calculus

The fractional or non-integer order calculus adds information to the classical calculus, with a more accurate description of certain natural phenomena. It can be applied in several areas of knowledge, such as physics, chemistry, engineering, technology, among others [5,7,14,12]. In this section we present two motivations for the use of fractional calculus: the Tautochrone problem and the effect of memory in biological models.

3.1 The Tautochrone problem

The tautochrone problem (or isochronic curve) corresponds to finding a curve s for which an object spends the same time to slide though the curve for any starting point y_0 to 0. The path is considered to be frictionless and under uniform gravity. In 1823, Abel solved this problem using fractional calculus. The equation that describes the object descent time is given by [1]

$$\tau = \frac{1}{\sqrt{2g}} \int_0^{y_0} (y - y_0)^{-\frac{1}{2}} \left(\frac{ds}{dy} \right) dy, \tag{11}$$

where g is gravity, $y(t)$ is the height of the object at time t, y_0 is the initial height at which the object was launched, and s is the desired curve given as a function of y [1].

The curve s can be find using the traditional calculus by applying the Laplace transform and the Convolution Theorem [1]. Abel obtained the same solution using fractional calculus, in particular, he observed that, except for the multiplication by $1/\Gamma(\frac{1}{2})$, Equation (11) corresponds to the fractional integral of order $\frac{1}{2}$ of the function $s'(y)$. Thus, one can easily obtain the desired solution if the fractional derivative of the constant τ is known [1].

3.2 Memory effect: traditional approach

As stated in Introduction, fractional calculus is a great tool that can be employed to describe real-life phenomena with so-called memory effect.

A classic models of autonomous ordinary differential equations have no memory, because their solution do not depend on the previous instant. For instance, if $f(t; x_0)$ is a solution of an autonomous first-order ordinary differential equation with the initial condition x_0 at $t = 0$, then we have the flow property $f(t + s; x_0) = f(t; f(s; x_0))$, which means that the solution does not change by considering $f(s; x_0)$ as initial condition since $f(s; x_0)$ belongs to the solution. Thus, given an initial value, the solution is uniquely determined for any point of domain. In general, this assertion is not true for fractional differential equations. One way to introduce the memory effect into a mathematical model is to change the order of the derivative of a classical model so that it is non-integer [2,13].

Let f be a real function defined in $[0,t]$, $t_1, t_2 \in [0,t]$ are such that $0 < t_1 < t_2$, and $H = (J^\alpha f)(t_2) - (J^\alpha f)(t_1)$ for $\alpha \in \mathbb{R}^+$. From equalities below, one can observe that the value of H depends on the entire range of f over $[0,t_2]$ if $\alpha \neq 1$, whereas H depends only on the range of f over $[t_1,t_2]$ if $\alpha = 1$:

$$\begin{aligned} H &= (J^\alpha f)(t_2) - (J^\alpha f)(t_1) \\ &= \frac{1}{\Gamma(\alpha)}\left[\int_0^{t_2}(t_2-s)^{\alpha-1}f(s)ds - \int_0^{t_1}(t_1-s)^{\alpha-1}f(s)ds\right] \qquad (12) \\ &= \frac{1}{\Gamma(\alpha)}\left[\int_{t_1}^{t_2}(t_2-s)^{\alpha-1}f(s)ds + \int_0^{t_1}\left[(t_2-s)^{\alpha-1}-(t_1-s)^{\alpha-1}\right]f(s)ds\right]. \end{aligned}$$

Note that if $\alpha = 1$, then the second integral is canceled:

$$H = \frac{1}{\Gamma(\alpha)}\int_{t_1}^{t_2}(t_2-s)^{\alpha-1}f(s)ds = \int_{t_1}^{t_2}f(s)ds, \qquad (13)$$

In contrast, the second integral is not canceled if $\alpha \neq 1$. From (12) we can see that H depends on what happens in $[0,t_1]$ and $[t_1,t_2]$. Thus, for $\alpha \neq 1$, H depends on the entire range of f over $[0,t_2]$. Therefore, the fractional integral in the interval $[t_1,t_2]$ is not uniquely determined, it depends on what happened before t_1 which characterizes the memory effect in the process.

Next, we study the memory effect in the fractional integral and in the derivatives of Liouville and Caputo. To this end, we use the notion of mathematical expectation which is a generalization of the arithmetic mean of observed data.

4 Statistical Approach

In this section we present the so-called memory effect in fractional calculus based on statistical expectation, to the best of our knowledge, which has not yet been presented in the literature. Here, we focus on the Riemann-Liouville integral and Riemann-Liouville and Caputo fractional derivatives of a f function.

4.1 Fractional operators

We begin this section with the proposition below, which characterizes three well-known fractional operators in terms of expected values of certain random variables. This result shows, in an objective way, the so-called memory effect in fractional calculus.

Proposition 4 *Let $\alpha \in \mathbb{R}^+$ and $f \in AC[0,b]$. Under these conditions, we have*

$$J_t^\alpha f(t) = \frac{t^\alpha}{\Gamma(\alpha+1)} E[f(tU)]; \tag{14}$$

$$D_t^\alpha f(t) = \frac{t^{-\alpha}}{\Gamma(1-\alpha)} E[f(tW)] + \frac{t^{1-\alpha}}{\Gamma(3-\alpha)} E\left[f'(tV)\right], \quad \textit{if } 0<\alpha<1; \tag{15}$$

$$cD_t^\alpha f(t) = \frac{t^{1-\alpha}}{\Gamma(2-\alpha)} E\left[f'(tW)\right], \quad \textit{if } 0<\alpha<1, \tag{16}$$

where U, V and W are random variables with the distributions $U \sim B(1,\alpha), V \sim B(2,1-\alpha)$ and $W \sim B(1,1-\alpha)$.

Proof First, note that $B(1,\alpha) = \dfrac{1}{\alpha}$.

From (2), we have

$$J_t^\alpha f(t) = \frac{1}{\Gamma(\alpha)} \int_0^t (t-s)^{\alpha-1} f(s)ds = \frac{1}{\Gamma(\alpha)} \int_0^t t^{\alpha-1} \left(1-\frac{s}{t}\right)^{\alpha-1} f(s)ds.$$

Let $u = \frac{s}{t}$, we obtain

$$\begin{aligned} J_t^\alpha f(t) &= \frac{t^\alpha}{\Gamma(\alpha)} \int_0^1 (1-u)^{\alpha-1} f(tu)du \\ &= \frac{t^\alpha B(1,\alpha)}{\Gamma(\alpha)} \int_0^1 \frac{(1-u)^{\alpha-1}}{B(1,\alpha)} f(tu)du \\ &= \frac{t^\alpha}{\alpha\Gamma(\alpha)} \int_0^1 \frac{(1-u)^{\alpha-1}}{B(1,\alpha)} f(tu)du. \end{aligned} \tag{17}$$

Using Item a) of Proposition 1 and the fact of $\dfrac{(1-u)^{\alpha-1}}{B(1,\alpha)}$ is the density function of a beta distribution, we have that (14) holds true for $U \sim B(1,\alpha)$.

Let $\alpha \in (0,1)$, from (17) we have

$$J_t^{1-\alpha} f(t) = \frac{t^{1-\alpha}}{\Gamma(1-\alpha)} \int_0^1 (1-u)^{-\alpha} f(tu)du.$$

Since $B(1,1-\alpha) = \dfrac{1}{1-\alpha}$ and $B(2,1-\alpha) = \dfrac{1}{(1-\alpha)(2-\alpha)}$, the product rule for derivatives reveals that

$$\begin{aligned} D_t^\alpha f(t) &= \frac{d}{dt}\left[J_t^{1-\alpha} f(t)\right] \\ &= \frac{(1-\alpha)t^{-\alpha}}{\Gamma(1-\alpha)} \int_0^1 (1-u)^{-\alpha} f(tu)du + \frac{t^{1-\alpha}}{\Gamma(1-\alpha)} \int_0^1 (1-u)^{-\alpha} uf'(tu)du \\ &= \frac{t^{-\alpha}}{\Gamma(1-\alpha)} \int_0^1 \frac{(1-u)^{-\alpha}}{B(1,1-\alpha)} f(tu)du + \frac{t^{1-\alpha}}{(1-\alpha)(2-\alpha)\Gamma(1-\alpha)} \int_0^1 \frac{(1-u)^{-\alpha}}{B(2,1-\alpha)} uf'(tu)du \\ &= \frac{t^{-\alpha}}{\Gamma(1-\alpha)} \int_0^1 \frac{(1-w)^{-\alpha}}{B(1,1-\alpha)} f(tw)dw + \frac{t^{1-\alpha}}{(1-\alpha)(2-\alpha)\Gamma(1-\alpha)} \int_0^1 \frac{v\,(1-v)^{-\alpha}}{B(2,1-\alpha)} f'(tv)dv \\ &= \frac{t^{-\alpha}}{\Gamma(1-\alpha)} E[f(tW)] + \frac{t^{1-\alpha}}{\Gamma(3-\alpha)} E[f'(tV)], \end{aligned}$$

where $W \sim B(1, 1-\alpha)$ and $V \sim B(2, 1-\alpha)$. Note that the beta function is well defined since $\alpha \in (0,1)$. Thus, we prove (15).

Finally, from (5), we have

$$\begin{aligned}
cD_t^\alpha f(t) &= J_t^{1-\alpha} f'(t) \\
&= \frac{1}{\Gamma(1-\alpha)} \int_0^t (t-s)^{-\alpha} f'(s) ds \\
&= \frac{1}{\Gamma(1-\alpha)} \int_0^t t^{-\alpha} \left(1 - \frac{s}{t}\right)^{-\alpha} f'(s) ds \\
&= \frac{1}{\Gamma(1-\alpha)} \int_0^1 t^{1-\alpha} (1-u)^{-\alpha} f'(tu) du \\
&= \frac{t^{1-\alpha}}{\Gamma(1-\alpha)} B(1, 1-\alpha) \int_0^1 \frac{(1-u)^{(1-\alpha)-1}}{B(1,1-\alpha)} f'(tu) du \\
&= \frac{t^{1-\alpha}}{(1-\alpha)\Gamma(1-\alpha)} \int_0^1 \frac{(1-w)^{(1-\alpha)-1}}{B(1,1-\alpha)} f'(tw) dw \\
&= \frac{t^{1-\alpha}}{\Gamma(2-\alpha)} E[f'(tW)], \qquad (18)
\end{aligned}$$

where $W \sim B(1, 1-\alpha)$. Thus, we conclude that (16) holds true.

Remark 2 Note that, by Definition 4, exchanging $f(t)$ for $f(t) - f(0)$, or equivalent $f(tW)$ for $f(tW) - f(0)$ in (15), for $0 < \alpha < 1$, we can write Caputo's derivative as

$$cD_t^\alpha f(t) = \frac{t^{-\alpha}}{\Gamma(1-\alpha)} E[f(tW) - f(0)] + \frac{t^{1-\alpha}}{\Gamma(3-\alpha)} E\left[f'(tV)\right]. \qquad (19)$$

We can see that (19) coincides with (16). This follows from the demonstration of Proposition 4 and Definitions (4) and (5).

Remark 3 Note that, for $0 < \alpha < 1, cD^\alpha f(t_\alpha) = 0$ does not imply t_α is a extremal point of f. In fact, suppose that f has just only local maximum t^*. In this case, we have $f'(s) > 0$ for all $s < t^*$ which implies that $E[f'(tW)] > 0$ for all $t \leq t^*$. Thus, if $E[f'(t_\alpha W)] = 0 \Leftrightarrow cD^\alpha f(t_\alpha) = 0$ then we must have that $t_\alpha > t^*$.

Next, we provide some examples of Riemann-Liouville and Caputo fractional derivatives using the formulas (15) and (16).

Example 1 If $f(t) = k$, where k is constant, we have $E[f(tW)] = E[k] = k$ and $E[f'(tV)] = E[f'(tW)] = E[0] = 0$. Thus, from (15) we have $D_t^\alpha f(t) = \dfrac{kt^{-\alpha}}{\Gamma(1-\alpha)}$, and from (16) we have $cD_t^\alpha f(t) = 0$.

Example 2 If $f(t) = t^\gamma$, with $\gamma \in (-1, \infty)$, we find $D_t^\alpha f(t)$ and $cD_t^\alpha f(t)$. Note that

$$\begin{aligned} E[f(tW)] &= \int_0^1 \frac{(1-w)^{-\alpha}}{B(1,1-\alpha)}(tw)^\gamma dw \\ &= t^\gamma(1-\alpha)\int_0^1 (1-w)^{-\alpha} w^\gamma dw \\ &= t^\gamma(1-\alpha)B(\gamma+1,1-\alpha), \end{aligned}$$

and

$$\begin{aligned} E[f'(tV)] &= \int_0^1 \frac{(1-v)^{-\alpha} v}{B(2,1-\alpha)}\gamma(tv)^{\gamma-1} dv \\ &= \frac{\gamma t^{\gamma-1}}{B(2,1-\alpha)}\int_0^1 (1-v)^{-\alpha} v^\gamma dv \\ &= \frac{\gamma t^{\gamma-1}}{B(2,1-\alpha)} B(\gamma+1,1-\alpha). \end{aligned}$$

From (7) and (15), we have

$$\begin{aligned} D_t^\alpha f(t) &= \frac{t^{-\alpha}}{\Gamma(1-\alpha)} t^\gamma(1-\alpha)B(\gamma+1,1-\alpha) + \frac{t^{1-\alpha}}{\Gamma(3-\alpha)}\frac{\gamma t^{\gamma-1}}{B(2,1-\alpha)} B(\gamma+1,1-\alpha) \\ &= \frac{(1-\alpha)t^{\gamma-\alpha}}{\Gamma(1-\alpha)} B(\gamma+1,1-\alpha) + \frac{\gamma t^{\gamma-\alpha}}{\Gamma(3-\alpha)B(2,1-\alpha)} B(\gamma+1,1-\alpha) \\ &= t^{\gamma-\alpha} B(\gamma+1,1-\alpha)\left[\frac{1-\alpha}{\Gamma(1-\alpha)} + \frac{\gamma}{\Gamma(3-\alpha)B(2,1-\alpha)}\right] \\ &= t^{\gamma-\alpha}\frac{\Gamma(\gamma+1)\Gamma(1-\alpha)}{\Gamma(2+\gamma-\alpha)}\left[\frac{1-\alpha}{\Gamma(1-\alpha)} + \frac{\gamma\Gamma(3-\alpha)}{\Gamma(3-\alpha)\Gamma(2)\Gamma(1-\alpha)}\right] \\ &= t^{\gamma-\alpha}\frac{\Gamma(\gamma+1)\Gamma(1-\alpha)}{\Gamma(2+\gamma-\alpha)}\left[\frac{1-\alpha}{\Gamma(1-\alpha)} + \frac{\gamma}{\Gamma(1-\alpha)}\right] \\ &= t^{\gamma-\alpha}\frac{\Gamma(\gamma+1)}{\Gamma(2+\gamma-\alpha)}\left[1+\gamma-\alpha\right] \\ &= t^{\gamma-\alpha}\frac{\Gamma(\gamma+1)}{(1+\gamma-\alpha)\Gamma(1+\gamma-\alpha)}\left[1+\gamma-\alpha\right] \\ &= t^{\gamma-\alpha}\frac{\Gamma(\gamma+1)}{\Gamma(1+\gamma-\alpha)}. \end{aligned} \tag{20}$$

Furthermore,

$$\begin{aligned} E[f'(tW)] &= \int_0^1 \frac{(1-w)^{-\alpha}}{B(1,1-\alpha)}\gamma(tw)^{\gamma-1} dw \\ &= \frac{\gamma t^{\gamma-1}}{B(1,1-\alpha)}\int_0^1 (1-w)^{-\alpha} w^{\gamma-1} dw \\ &= \frac{\gamma t^{\gamma-1}}{B(1,1-\alpha)} B(\gamma,1-\alpha). \end{aligned}$$

Replacing in (16), we obtain

$$\begin{aligned} cD_t^\alpha f(t) &= \frac{t^{1-\alpha}}{\Gamma(2-\alpha)} \frac{\gamma t^{\gamma-1}}{B(1,1-\alpha)} B(\gamma, 1-\alpha) \\ &= \frac{t^{1-\alpha}}{\Gamma(2-\alpha)} \frac{\gamma t^{\gamma-1}\Gamma(2-\alpha)}{\Gamma(1)\Gamma(1-\alpha)} \frac{\Gamma(\gamma)\Gamma(1-\alpha)}{\Gamma(1+\gamma-\alpha)} \\ &= t^{1-\alpha} t^{\gamma-1} \frac{\gamma\Gamma(\gamma)}{\Gamma(1+\gamma-\alpha)} \\ &= t^{\gamma-\alpha} \frac{\Gamma(\gamma+1)}{\Gamma(1+\gamma-\alpha)}. \end{aligned} \tag{21}$$

The results of Examples 1 and 2 coincide with those presented in the literature, showing that the equations (15) and (16) can be used instead of the traditional approach to fractional calculus. Moreover, in Example 2, the equations (20) and (21) are the same, which is correct since $D_t^\alpha f(t) = cD_t^\alpha f(t)$ for $f(0) = 0$ and for all $\alpha \in (0, 1)$ (see Equation (19)).

4.2 The memory effect and hysteresis phenomenon

The memory effect on fractional operators is clear from formulas (14) - (16). By the way, we attest the presence of such an effect in the formula (14). The other operators have similar explanations.

Since U has distribution $B(1, \alpha)$, the random variable $S = tU$ assumes the values in the inteval $(0, t)$. Thus, from (14), $J_t^\alpha f(t)$ coincides with $\frac{t^\alpha}{\Gamma(\alpha+1)} E[f(S)]$, $0 \leq s \leq t$. Clearly, $J_t^\alpha f(t)$ is affected by all prior values at t because the expected value $E[f(S)]$ is. Since $E[f(S)]$ appears in (15) and (19), it follows that $D_t^\alpha f(t)$ and $cD_t^\alpha f(t)$ also have a memory effect.

The formulas (14)-(16) reveal interesting interpretations:

1) The fractional integral $J_t^\alpha f(t)$ is proportional to the average of $f(s)$, considering all prior values s at t;
2) $D_t^\alpha f(t)$ is the classic derivative of an amount proportional to the average of the $f(s)$ and $f'(s)$ functions, considering all prior values s at t;
3) $cD_t^\alpha f(t)$ is proportional to the average of the classic derivative $f'(s)$, considering the all values s less than t;
4) If $\alpha = 1$, then $U \sim B(1, 1)$, that is, U has uniform distribution so that $J_t^\alpha f(t) = tE[f(tU)] = \int_0^t f(s)ds$. Thus, $D_t^\alpha f(t) = \dfrac{d}{dt} J_t^0 f(t) = \dfrac{d}{dt} f(t) = f'(t)$ and $cD_t^\alpha [f(t) - f(0)] = \dfrac{d}{dt} J_t^0 [f(t) - f(0)] = \dfrac{d}{dt}[f(t) - f(0)] = f'(t)$. Consequently, the fractional calculus coincides with the classic one, when $\alpha = 1$.

A phenomenon given by a certain physical/chemical/biological system of which the properties of the present depend on its previous history is called *hysteresis*. Items 1), 2) and 3) indicate that the values of the fractional integral,

as well as the fractional derivatives in t, are affected by the historical values of f (at every time before t). Thus, the fractional calculus seems to be a more adequate mathematical tool for modeling phenomena with hysteresis than the classical calculus (that is, for the case where $\alpha = 1$).

4.3 Influence of Beta distribution on fractional operators of order α

Since each historical value (before t) acts differently for fractional operators, according to the distributions $B(1,\alpha), B(1,1-\alpha)$ and $B(2,1-\alpha)$, we investigate which ones contribute most to these operators with respect to the order $\alpha \in (0,1)$.

According to the formula (14), the value of $J_t^\alpha f(t)$ is affected according to the density $f_U(u) = \dfrac{(1-u)^{\alpha-1}}{B(1,\alpha)}$, which is increasing if $0 < \alpha < 1$ and decreasing if $\alpha > 1$. For $0 < \alpha < 1$, recent values (*i.e.*, close to $t \Leftrightarrow u \simeq 1$) contribute more to the fractional integral $J_t^\alpha f(t)$ than the remote ones (*i.e.*, close to $0 \Leftrightarrow u \simeq 0$). On the other hand, for $\alpha > 1$ the opposite occurs.

From the formulas (15) and (16), one can note that Riemann-Liouville and Caputo derivative operators have similar influence of prior values of f to the integral for $0 < \alpha < 1$. In particular, values close to t contribute more to fractional derivatives than remote values (those ones evaluated for times close to 0). This is due to the fact that density distributions $f_W(w) = \dfrac{(1-w)^{-\alpha}}{B(1,1-\alpha)}$ and $f_V(v) = \dfrac{v\,(1-v)^{-\alpha}}{B(2,1-\alpha)}$ are increasing for $0 < \alpha < 1$.

For the integral operator, the higher the value of $\alpha \in (0,1)$, the more uniform are the weights of the initial and final values, that is, the closer to the uniform distribution the random variable U becomes. For derivative operators, the opposite occurs. This is illustrated in Figure 1. Note that the density function $f_U(\cdot)$, for the parameter α, is equal to the density function $f_W(\cdot)$ for the parameter $1-\alpha$. The $f_V(\cdot)$ density function follows the same pattern as $f_W(\cdot)$, but with more accentuated increase.

Regarding the fractional integral, we have that the higher the value of α the greater the contribution of remote values ($u \simeq 0$). In contrast, the higher α, the smaller the contribution of the values evaluated close to t (*i.e.*, $u \simeq 1$). With respect to the Riemann-Liouville and Caputo fractional derivative operators, we obtain an opposite behaviour.

Next, we admit the effect of hysteresis in an epidemiological SIR model in order to study the Covid-19 in four countries: South Korea, China, Switzerland, and Spain.

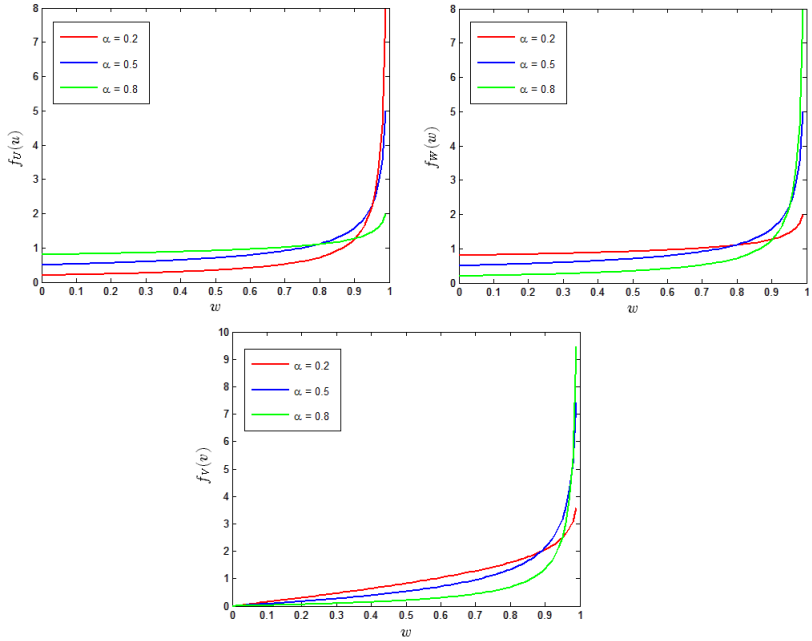

Fig. 1 Density functions f_U, f_W and f_V, for parameters $\alpha = 0.2, \alpha = 0.5$ and $\alpha = 0.8$. a) shows the distribution of historical weights for fractional integral; b) illustrates the distribution of historical weights for the Caputo and Riemann-Liouville derivatives; c) shows the distribution that, combined with f_W, defines the historical weights for the Riemann-Liouville derivative.

5 Application

In this section we analyze the spread of Covid-19 in some countries using an epidemiological model of the SIR type. This is a simple compartmental model that was proposed in 1927 by Kermack and McKendrick [6] and is widely used to study the evolution of some diseases. In [10], the authors pointed out that the hysteresis phenomenon should ideally be considered in the analysis of the epidemiological behaviour of diseases due to actions caused by the protective instinct and immunity, that are influenced respectively by memory and the so-called immune memory of the body. Since we desire to incorporate the memory effect characterized by hysteresis phenomenon, we use the fractional version of the SIR model.

5.1 The models

In the epidemiological SIR model, the population is divided into three compartments: susceptible, infected , and recovered. Susceptible individuals correspond to those exposed to the disease, but not yet infected. Who have already been infected but are no longer infected and have gained immunity are classi-

fied as recovered. Originally, the model is given by

$$\begin{cases} S'(t) = & -\beta SI \\ I'(t) = & \beta SI - \gamma I\,, \\ R'(t) = & \gamma I \end{cases} \tag{22}$$

where $S(t), I(t)$ and $R(t)$ are the number of susceptible, infected, and recovered individuals at instant t, respectively. β is the infection rate and γ is the recovery rate [4,6].

In this work, we analyze the classical and fractional versions of the SIR model. The fractional version is given as follows:

$$\begin{cases} cD_t^\alpha S(t) = & -\beta SI \\ cD_t^\alpha I(t) = & \beta SI - \gamma I\,, \\ cD_t^\alpha R(t) = & \gamma I \end{cases} \tag{23}$$

where $cD_t^\alpha X(t)$ is the fractional derivative of Caputo, according to the Definition 4, of order $\alpha \in (0,1)$. We consider $\beta, \gamma \in (0,1)$.

5.2 Methodology and numerical solution

In order to compare the classic and fractional SIR models given respectively in (22) and (23), we take data from active cases of the Covid-19 disease, that is, cases of infected people at the analyzed moment, not accumulated [17], in each of the countries: South Korea, China, Switzerland and Spain. We consider the numerical solutions for wich the functions I of the number of infected which best fit the real data.

The parameters β, γ and, in the fractional case, α, are obtained by minimizing the mean squared error:

$$\sum_{i=1}^{n} (I(t_i) - obs(t_i))^2, \tag{24}$$

where *obs* is the vector with n real data about Covid-19. The adjustment is performed twice, one for the model (22), with $\alpha = 1$ and other for the model (23), where the 3 parameters are found together. Thus, the values β and γ obtained for (22) may be different from those found for (23).

The data are normalized, that is, the values of *obs* are divided by the value N of the initial susceptible population, so that the data now represent the proportion of infected people and the size of the population of the country becomes 1. For selected countries, we consider N to be the number of inhabitants of the country divided by 10^2 or 10^3, since initially we do not have the entire population of the country being susceptible, but only the regions where the first cases occur. This was done since the SIR model may not be effective in describing the behavior of the disease if the population considered is much larger than that potentially affected. For example, if the size of the total population of country is much larger than the maximum value of its available data,

the peak solution for both (22) and (23) models is much larger than the data peak. This produces a difference in scale that impairs the visualization of the fit of the models to the data.

The initial condition (S_0, I_0, R_0) is given equally for the two both models (22) and (23), considering I_0 equal to the first value of the normalized real data and $R_0 = 0$. Since this model does not consider vital dynamics, we have $1 = S + R + I$ and, therefore, $S_0 = 1 - I_0$. The numerical solution is obtained using the Adams-Bashforth-Moulton PECE predictor-corrector method [3].

5.3 Results

In this section, we present the results obtained with the models for the number of infected by Covid-19 for four countries. It is worth pointing out that the objective of this work is to analyze the effectiveness of the SIR models (22) and (23) using Covid-19 data. However, we do not intend to make predictions about the evolution of the disease. The graphs in Figures 2-5 show the real data in blue dotted line, the red dashed lines represent the solution of the fractional model (that is, with memory), and the black continuous lines are the solutions of the classic model. Finally, Table 1 exhibits the mean squared errors (24) obtained of each model and country as well as the corresponding fractional order α. Tables 2 and 3 present the parameters used in our simulations.

In Figure 2, we can observe the behavior of the infected curve obtained by both models, (22) and (23), in comparison to the real data of Covid-19 in South Korea from February 15 to May 31, 2020, where we consider $N = 52000$.

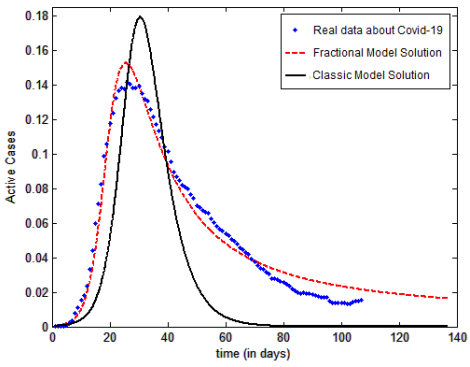

Fig. 2 Solutions of the (22) and (23) models in the description of the spread of Covid-19 in South Korea. For the model (22), we use $\beta = 0.5041$ and $\gamma = 0.2344$. For the model (23), we use $\beta = 0.8500$, $\gamma = 0.3869$, and $\alpha = 0.7081$.

Note that the data curve is flatter and wider than that given by the classic SIR model. In this case, the fractional solution fits better the data due to the freedom of the parameter α (that is associated with memory effect). In

this example, we can see how the fractional model contributes to a better description of the phenomenon. Table 1 corroborates this fact, showing that the mean squared error obtained by the fractional models is less than the one obtained by the classic models.

Figure 3 shows the solutions of the fractional and classic models in comparison to the Covid-19 data of China from January 22 to May 31, 2020. In these simulations, we consider $N = 140000$.

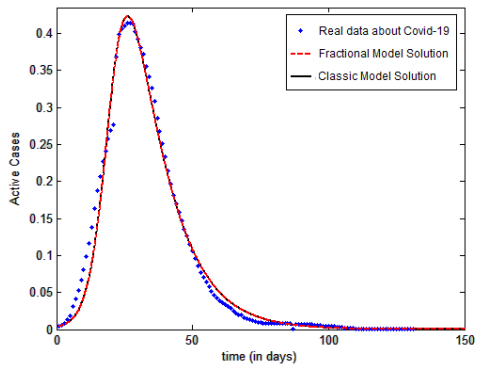

Fig. 3 Solutions of the (22) and (23) models in the description of the spread of Covid-19 in China. We use $\beta = 0.3559$ and $\gamma = 0.0842$ for both models and $\alpha = 0.9999$ for the fraction model.

In Figure 3, the fractional model (23) did not present much difference from the classic model (22). In fact, we can see in Table 1 that the mean squared errors is the same for both models.

In Figure 4, we compare the models by analyzing the disease data in Switzerland from February 25 to May 31, 2020, where we consider $N = 90000$.

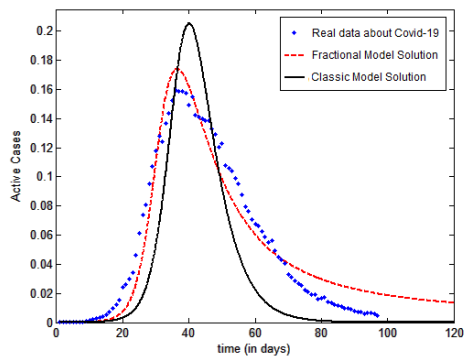

Fig. 4 Solutions of the (22) and (23) models in the description of the spread of Covid-19 in Switzerland. For the model (22), we use $\beta = 0.5245$ and $\gamma = 0.2267$. For the model (23), we use $\beta = 0.7536$, $\gamma = 0.3274$, and $\alpha = 0.7726$.

Again, in Figure 4, we can note that the fractional model fits the data better than the classic one. This can also be observed in Table 1. The blue dotted curve is wider with a slower decay than the one produced by the classic SIR model. This fact can best be modeled when there is a memory effect.

In Figure 5, we compare the models using data of Italy from February 15 to May 31, where we consider $N = 600000$. From Table 1, we can observe that this is another example where the use of the fractional model yielded solutions with mean squared error less than the one produced by the classical model.

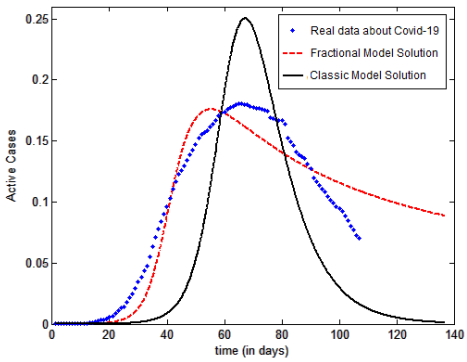

Fig. 5 Solutions of the (22) and (23) models in the description of the spread of Covid-19 in Italy. For the model (22), we use $\beta = 0.3105$ and $\gamma = 0.1186$. For the model (23), we use $\beta = 0.7764$, $\gamma = 0.3069$, and $\alpha = 0.5514$.

It is worth noting that the peaks obtained (in $t = \bar{t}$) with the solutions of the model (23) is closer to reality than the solutions of the model (22) in all countries. Moreover, each peak is on the left that one of (22) according to Remark 3, since $cD^{\alpha}I(\bar{t}) = 0$ for all $0 < \alpha < 1$.

Table 1 exhibits the mean squared errors calculated according to Equation (24) for the classical and fractional models with respect to the Covid-19 data from South Korea, China, Switzerland, and Spain. For each country, the order α obtained for the fractional derivative is also shown in Table 1.

Table 1 Mean squared errors achieved by the classical and fractional models and the corresponding order α of the fractional derivative for each country.

	China	Switzerland	S. Korea	Italy
Solution error of classic model	0.0290	0.0903	0.1175	0.3024
Solution error of fractional model	0.0290	0.0160	0.0052	0.0291
Fractional derivative order (α)	0.9999	0.7726	0.7081	0.5514

Finally, Tables 2 and 3 present the parameters used for the models (22) and (23) for each country.

Table 2 Parameters of classical model (22).

	China	Switzerland	South Korea	Italy
Infection rate β	0.3559	0.5245	0.5041	0.3105
Recovery rate γ	0.0842	0.2267	0.2344	0.1186

Table 3 Parameters of fractional model (23).

	China	Switzerland	South Korea	Italy
Infection rate β	0.3559	0.7536	0.8500	0.7764
Recovery rate γ	0.0842	0.3274	0.3870	0.3069
Derivative order α	0.9999	0.7726	0.7081	0.5514

5.4 Numerical solutions for weighted data

In this section illustrates the comments made in Subsection 4.3 regarding the influence of data on the fractional operators and the fractional order α, for $0 < \alpha < 1$. Here, the methodology for finding numerical solutions is analogous to the one described in Subsection 5.2, but we modify the formula (24) as follows:

$$\sum_{i=1}^{n} w_i[(I(t_i) - obs(t_i))^2], \tag{25}$$

where $w_i \in \mathbb{R}$ is the weight assigned to the data. Here, we adopt

(i) $w_i = \dfrac{2(n+1-i)}{n(n+1)}$, $i = 1, \ldots, n$, when the greatest weight is attributed to the first data.

(ii) $w_i = \dfrac{2i}{n(n+1)}$, $i = 1, \ldots, n$, when the greatest weight is attributed to the latest data;

In order to illustrate the influence of these weights on the model (23), we focus only on data from Switzerland.

In Subsection 4.3 we argue that if the order α of the Caputo derivative is higher, then the contribution of the latest data ($u \simeq 1$) is higher. On the other hand, if the value of α is lower, then the contribution of the first data ($u \simeq 0$) is higher.

In our simulations in the Subsection 5.3 for Switzerland, we obtain $\alpha = 0.6149$ as the fractional order of the derivative, according to the model (23). By considering the weigths w_i given as in Item (i), that is, the highest weights attributed to the first data, we obtain $\alpha = 0.5596$ as the order of the derivative for the fractional model. As expected, the value of the derivative order decreased. Figure 6 exhibtis the numerical solution for this case.

In Figure 7, the parameters are adjusted with the highest weight attributed to the latest data, that is, according Item (ii). In this case, we obtain $\alpha = 0.6310$ for the derivative order of the fractional model. Again as expected, the value α increased in comparison to the adjustment made in Subsection 4.3.

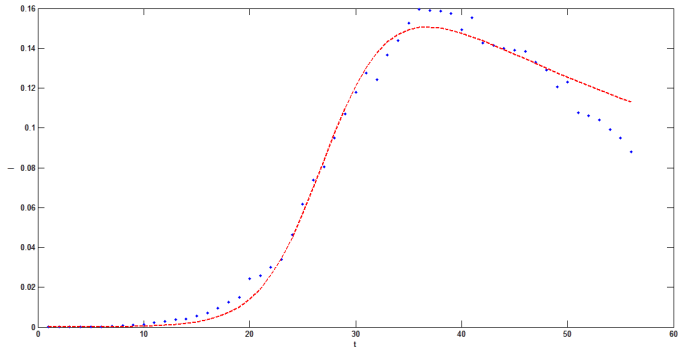

Fig. 6 Solution of the model (23) with parameter estimation using weights given as in Item (i).

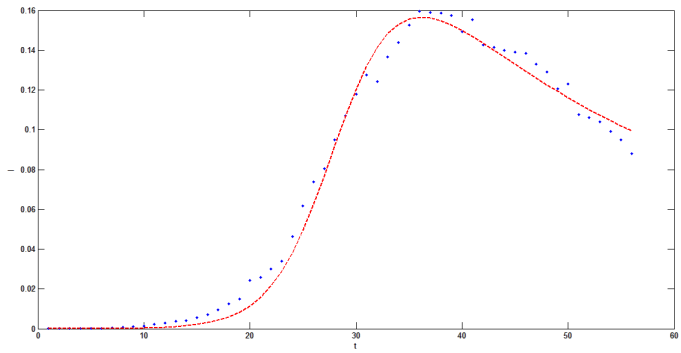

Fig. 7 Solution of the model (23) with parameter estimation using weights given as in Item (ii).

6 Discussions and Conclusions

In this work we have verified, under statistic point of view, the memory effect in the fractional calculus. We have shown that both fractional integral and derivative of a function f in instant t are, respectively, proportional to average of $f(s)$ of the function and its classical derivative $f'(s)$, for all instants s between zero and t. So, in fact, the fractional calculus is an appropriate methodology to treat dynamical systems with memory. From this approach we also proved the loss of the memory effect when $\alpha = 1$ in $(14) - (16)$, that is, when we return to the classic case. Moreover, since memory effect involves all history before the present instant, that is, it considers all times s from 0 to t, factional calculus can be viewed as a suitable tool for modeling of phenomenon with hysteresis. The hysteresis phenomenon can be seen in several dynamic systems, such as physical or biological systems, for which important properties depend on their previous history.

In addition, we show the contribution of the function values to the fractional operators is higher or lower according to the order of the operator. In

particular, the final values of the function have greater influence on the values of the fractional Riemann-Liouville and Caputo derivatives for $0 < \alpha < 1$.

We illustrate the use of a fractional model to model a system with memory using a simple compartmental SIR model which is a well-known and applicable model in epidemiology. Specifically, we study Covid-19 disease by assuming that it obeys the dynamics of the SIR epidemiologic model. For the purpose of comparing the results obtained via fractional calculus and via classical calculus, we study the evolution of Covid-19 disease in four countries, namely South Korea, China, Switzerland, and Spain. The results for these countries show that the fractional calculus produced more satisfactory results than those obtained using the classical theory.

Conflict of interest

The authors declare that they have no conflict of interest.

References

1. Camargo, R. F. Oliveira, E. C., Cálculo Fracionário. Livraria da Física, São Paulo (2015).
2. Diethelm, K., The Analysis of Fractional Differential Equations: An application-oriented exposition using differential operators of Caputo type. Springer Science & Business Media (2010).
3. Diethelm, K. Freed, A.D. The Frac PECE subroutine for the numerical solution of differential equations of fractional order, Forschung und Wissenschaftliches Rechnen 1998. Gessellschaft fur Wissenschaftliche Datenverarbeitung, Gottingen, pp. 57-71 (1999).
4. Edelstein-Keshet, L., Mathematical Models in Biology. Random House (1988).
5. Herrmann, Richard., Folded potentials in cluster physics-a comparison of Yukawa and Coulomb potentials with Riesz fractional integrals, Journal of Physics A: Mathematical and Theoretical, 46, 405-203 (2013).
6. Kermack, W. O., McKendrick, A. G., A contribution to the mathematical theory of epidemics, Proceedings of the royal society of London. Series A, Containing papers of a mathematical and physical character, 115.772, 700-721 (1927).
7. Li, Yuan-lu, Hui-qiang Tang, and Hai-xiu Chen., Fractional-order derivative spectroscopy for resolving simulated overlapped Lorenztian peaks, Chemometrics and Intelligent Laboratory Systems, 107, 83-89 (2011).
8. Lopes, M. M., Dinâmica da Propagação de Memes via Sistemas com Memória, Dissertation, University of Alfenas (2019). In Portuguese.
9. Mood, A. M. Graybill, F. A., Introduction to the Theory of Statistics. McGraw - Hill Book Company (1974).
10. Pimenov, A., et al., Memory effects in population dynamics: spread of infectious disease as a case study, Mathematical Modelling of Natural Phenomena, 7, 204-226 (2012).
11. Pinto, C. Tenreiro Machado, J. A. Fractional dynamics of computer virus propagation. Mathematical Problems in Engineering, 2014.
12. Saad, K. M. Baleanu, D. Atangana, A. New fractional derivatives applied to the Korteweg–de Vries and Korteweg–de Vries–Burger's equations. Computational and Applied Mathematics, 37(4), 5203-5216, 2018.
13. Saeedian, M., et al., Memory effects on epidemic evolution: The susceptible-infected-recovered epidemic model, Physical Review, 95, 0224091-0224099 (2017).
14. Silva, Manuel F., JA Tenreiro Machado, and A. M. Lopes., Fractional order control of a hexapod robot, Nonlinear Dynamics, 38, 417-433 (2004).
15. Srivastava, H. M. Saxena, R. K. Operators of fractional integration and their applications. Applied Mathematics and Computation, 118(1), 1-52, 2001.

16. Teodoro, G. S., Oliveira, D. S., Oliveira, E. C., Sobre derivadas fracionárias, Revista Brasileira de Ensino de Física, 40, 23071-230726 (2018).
17. Worldometers. "Coronavirus". Worldometers Website. Available in: `https://www.worldometers.info/coronavirus` (Accessed 02 June 2020).

Figures

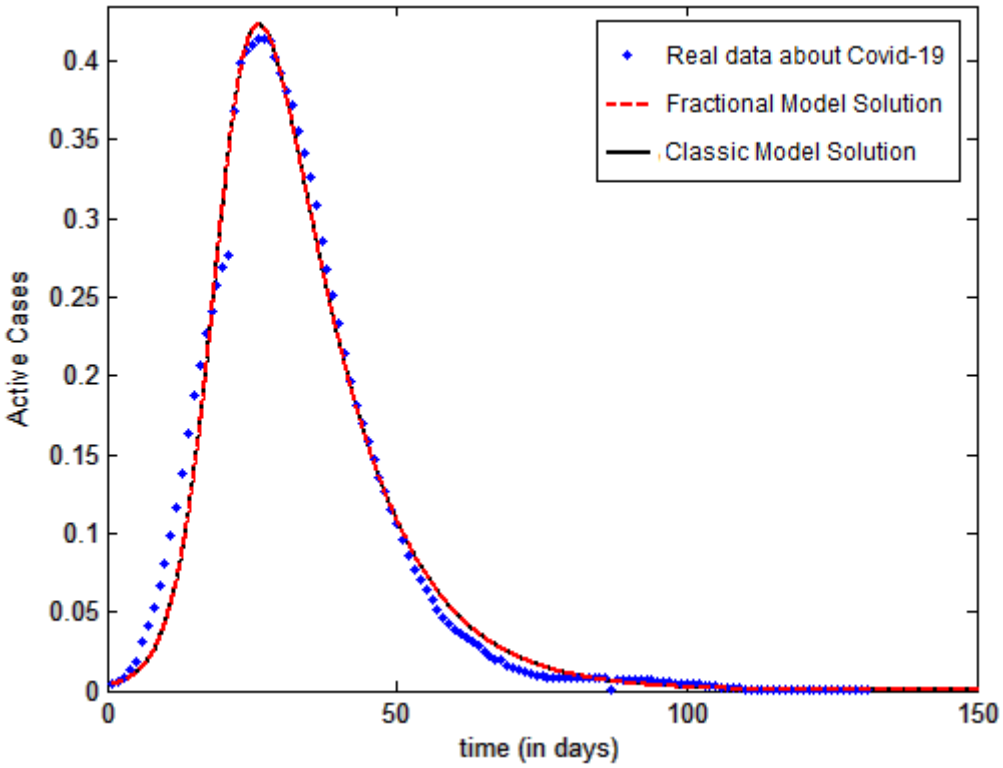

Figure 1

Model solutions with ordinary and fractional differential equations to describe the spread of Covid-19 in China.

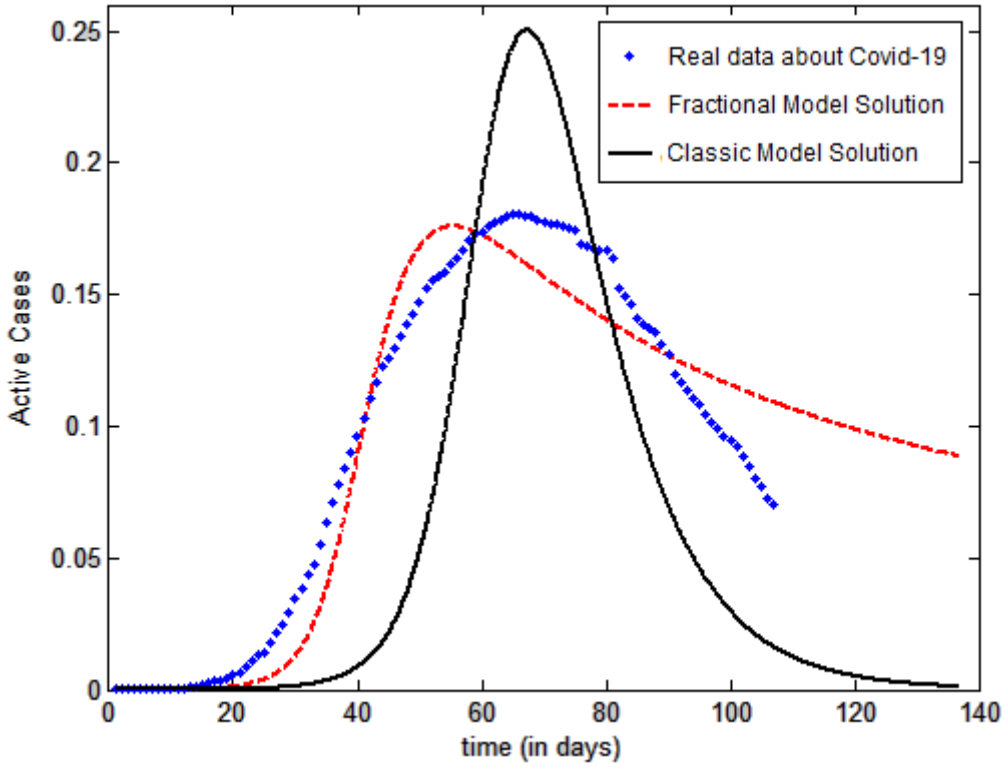

Figure 2

Model solutions with ordinary and fractional differential equations to describe the spread of Covid-19 in Italy.

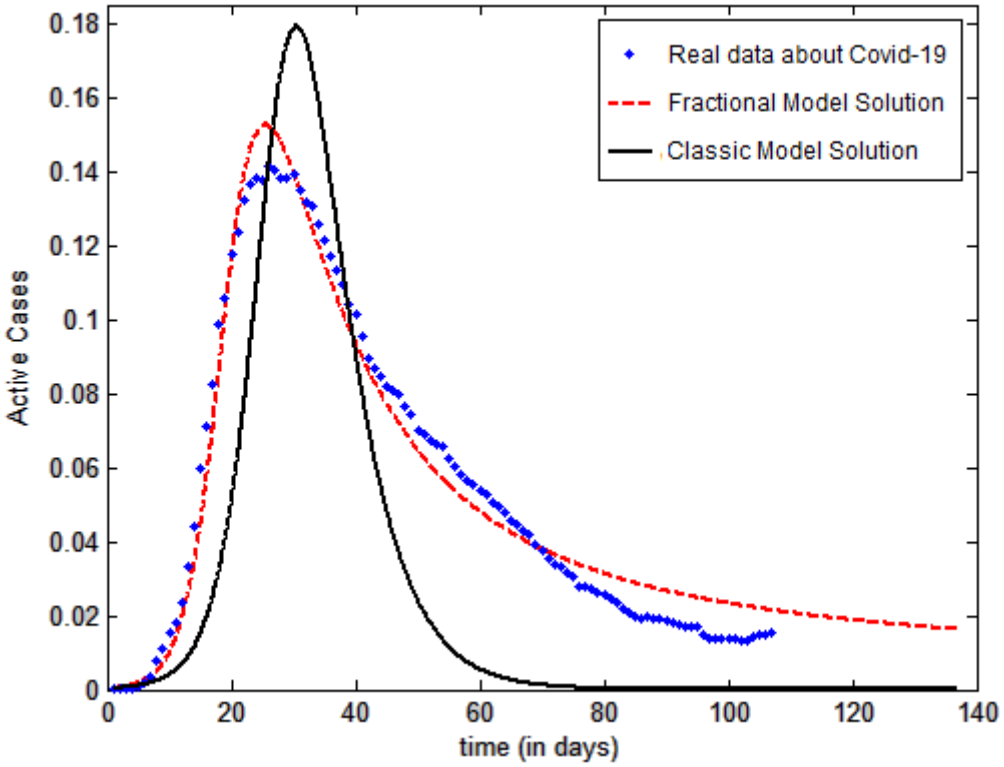

Figure 3

Model solutions with ordinary and fractional differential equations to describe the spread of Covid-19 in South Korea.

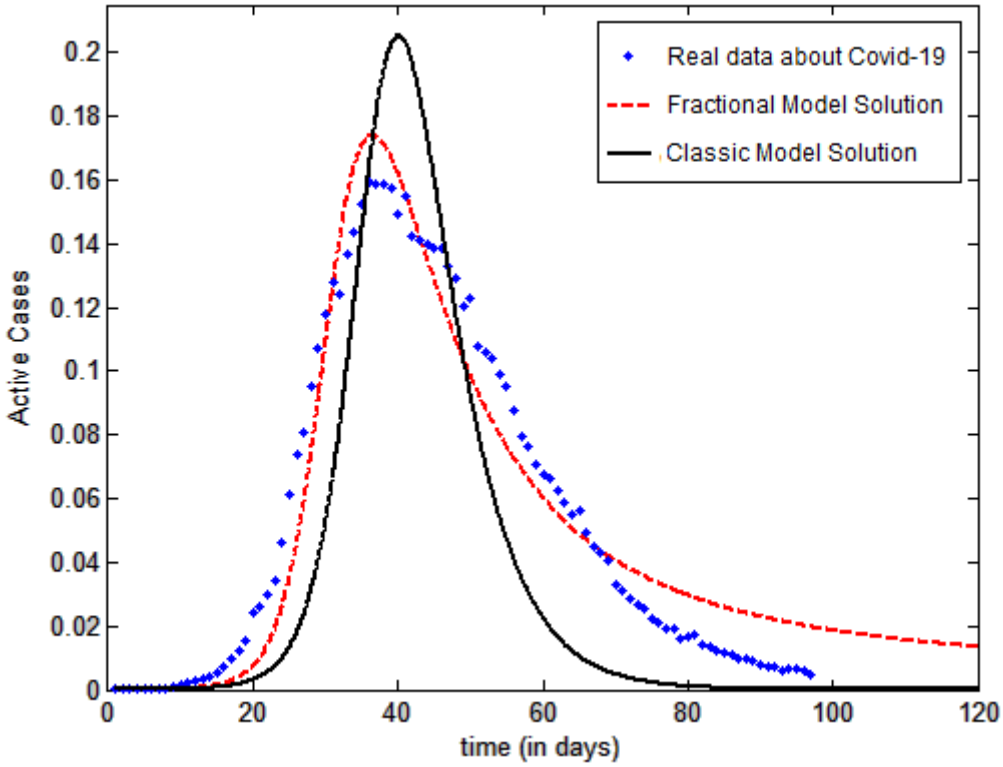

Figure 4

Model solutions with ordinary and fractional differential equations to describe the spread of Covid-19 in Switzerland.

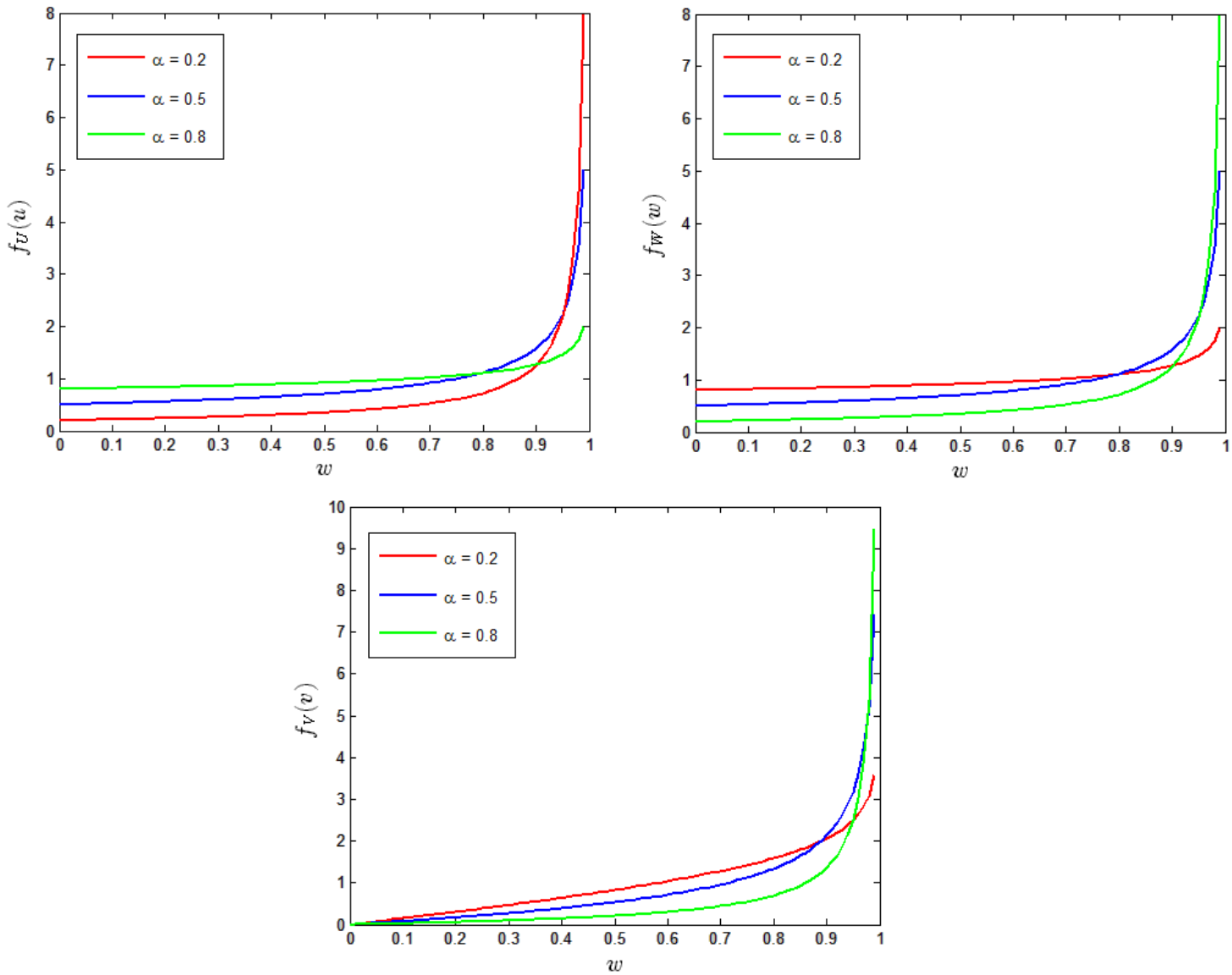

Figure 5

Density functions for different parameter values. a) shows the distribution of historical weights for fractional integral; b) illustrates the distribution of historical weights for the Caputo and Riemann-Liouville derivatives; c) shows the distribution that, combined with b) defines the historical weights for the Riemann-Liouville derivative.

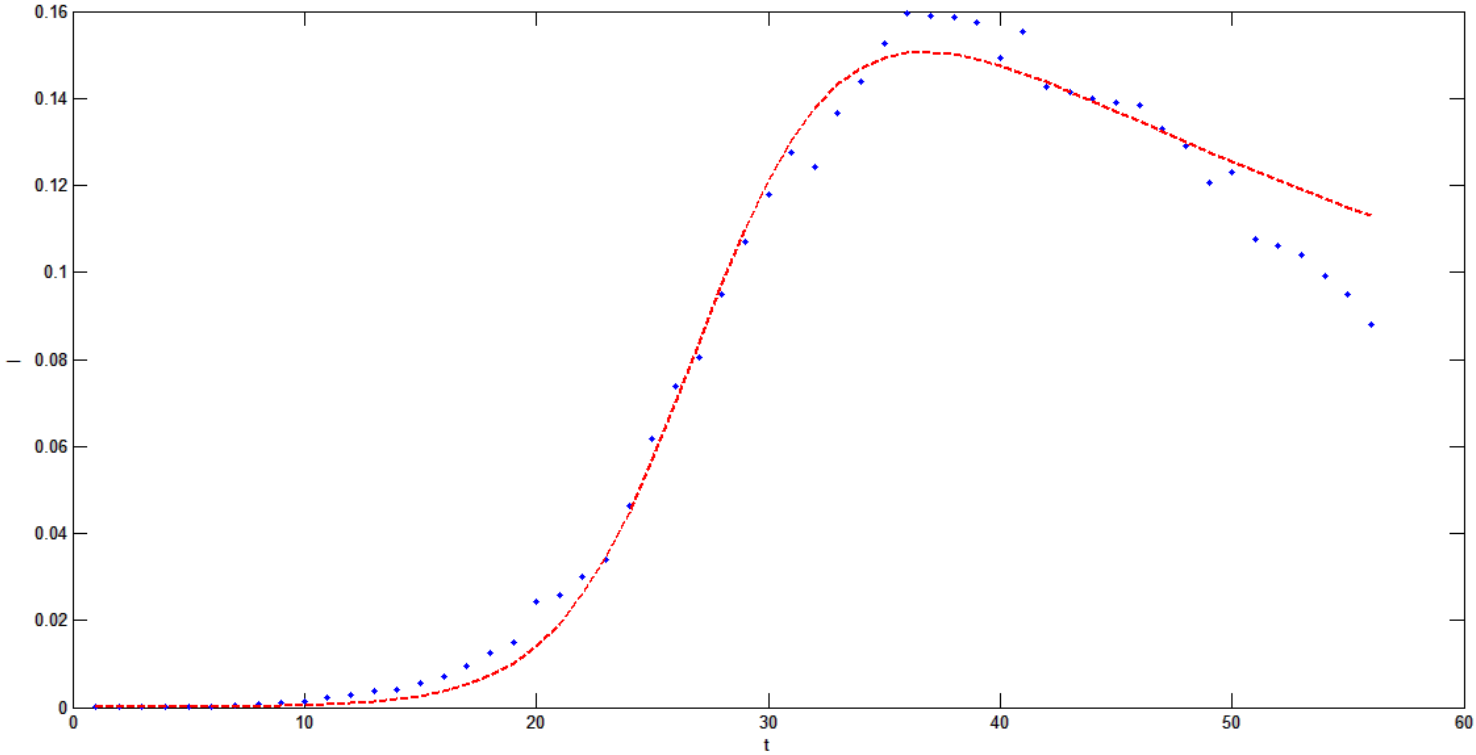

Figure 6

The fractional model solution with parameter estimation giving greater weight to the first data.

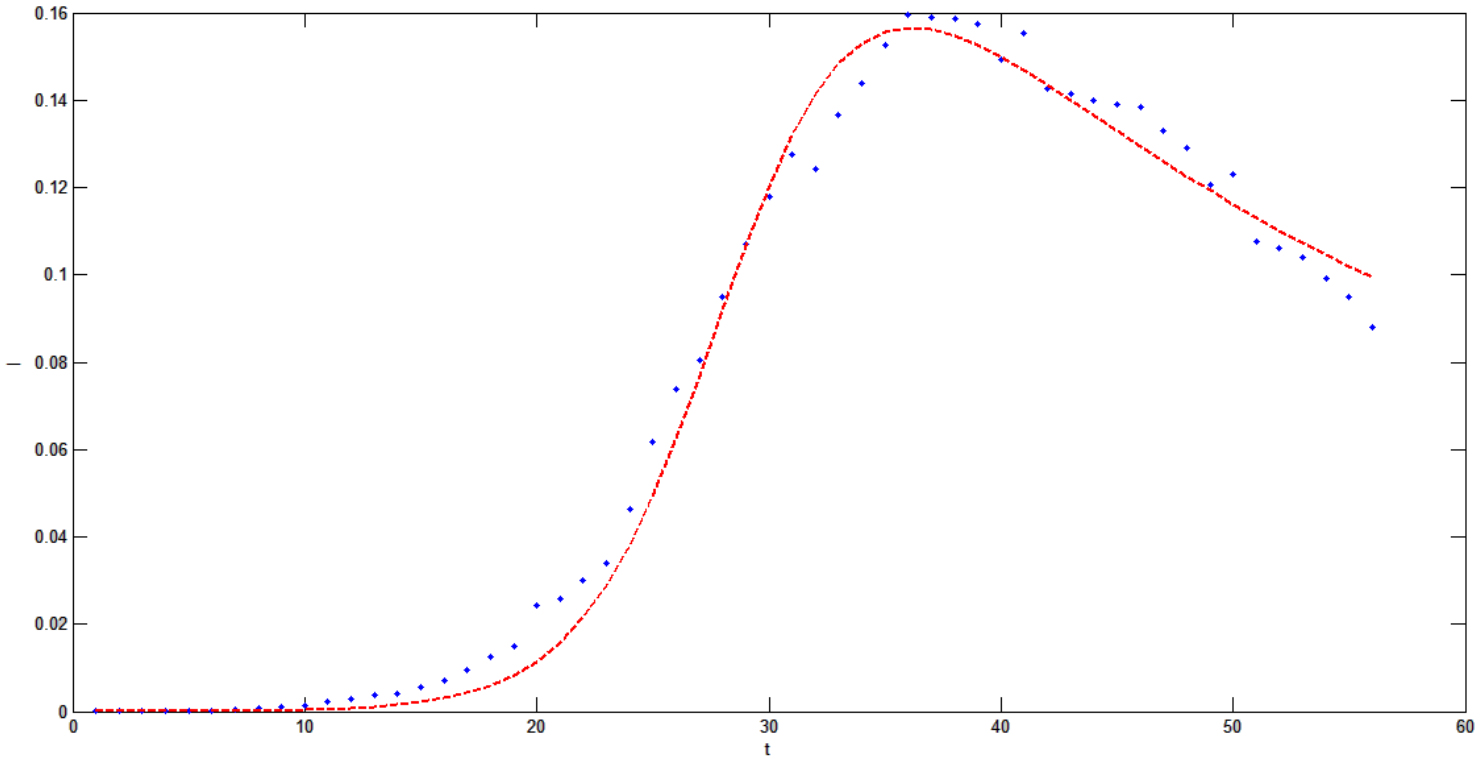

Figure 7

The fractional model solution with parameter estimation giving greater weight to the latest data.